X-ray diagnostics of fast electrons propagation in high density plasmas obtained by cylindrical compression

B Vauzour[1], M Koenig[2], D Batani[3], S Baton[2], F N Beg[4], C Benedetti[5], E Brambrink[2], S Chawla[4], F Dorchies[1], C Fourment[1], M Galimberti[6], L A Gizzi[7], R Heathcote[6], D P Higginson[4], S Hulin[1], R Jafer[3], P Köster[7], L L Labate[7], K L Lancaster[6], A J MacKinnon[8], A G MacPhee[8], W Nazarov[9], Ph Nicolaï[1], J Pasley[10], F Perez[2], X Ribeyre[1], M Richetta[11], J J Santos[1], G Schurtz[1], A Sgattoni[5], C Spindloe[6], L Volpe[3]

1 Centre Lasers Intenses et Applications, Université Bordeaux 1-CNRS-CEA, 33405 Talence, France
2 Laboratoire pour l'Utilisation des Lasers Intenses, 91761 Palaiseau, France
3 Dipartimento di Fisica, Università degli Studi di Milano-Bicocca, 20126 Milan, Italy
4 University of California, San Diego, La Jolla, USA
5 Dipartimento di Fisica, Università di Bologna, Italy
6 Central Laser Facility, Rutherford Appleton Laboratory, Didcot, UK
7 LIL-IPCF, Consiglio Nazionale delle Ricerche, Pisa, Italy
8 Lawrence Livermore National Laboratory, USA
9 University of St Andrews, Fife KY16 9AJ, Scotland
10 Department of Physics, University of York, YO10 5DD, UK
11 Dipartimento di Ingeneria Meccanica, Università di Roma Tor Vergata, Italy

E-mail: Santos.Joao@celia.u-bordeaux1.fr

Abstract. We report on X-ray diagnostics results from an experiment on fast electrons propagation in cylindrically compressed targets. It was performed on the VULCAN TAW laser facility at RAL (UK) using four long pulses (1ns, 70 J each at 2ω) to compress a cylindrical polyimide target filled with CH foam at 3 different initial densities. The cylindrical geometry allows us to reach temperatures and densities higher than those obtained in planar geometry compression. 2D hydrodynamic simulations predicted a core density range from 4 to 8 g/cm^3 and a core temperature from 30 eV up to 175 eV at maximum compression. An additional short laser pulse (10 ps, 160 J at ω) was focused on a Ni foil at one of the cylinder edges in order to generate a fast electrons current propagating along the compressed target. A X-ray radiography diagnostic was implemented in order to estimate the core plasma conditions of the compressed cylinder. Moreover two Bragg X-ray spectrometers collected the Kα fluorescence from the target so as to determine the variations of fast electrons population during the compression.

1. Introduction

In the context of the fast ignition scheme, a high energy electrons current produced by an ultra-intense laser beam heats highly compressed DT plasma. The fast electrons, produced near the

critical density, must propagate over a few 100 μm of overdense plasma and deposit their energy ($\approx$ 10 kJ) into the high density fuel [1]. In order to predict and understand the fast electron generation and transport some experiments have been successfully carried out on solid targets. However in this case the achieved densities and temperatures are lower than those expected for the fast ignition [2]. Such differences may involve some modifications in the predicted behaviour of the electrons such as their stopping power or their divergence in the compressed matter.
An alternative geometry consist in radially compress a cylindrical target [3]. It is thus possible to obtain plasmas with densities 10 times greater than the solid density and temperatures of a few hundreds eV. In fast ignition experiments this state of matter well known as warm and dense matter (WDM) is representative of the coronal plasma near the fast electron source and also presents a similar level of degeneracy of the compressed fuel. Using this geometry we have thus performed an experiment on the Vulcan TAW laser facility at RAL. The experiment was split in two phases. A first phase consisted in studying the cylindrical target compression to evaluate the targets' core densities and temperatures profiles at different moments of the implosion. A second phase was devoted to study the fast electrons propagation in such compressed targets.

2. Experimental setup

Four long pulse (LP) laser beams (4×70 J, 1ns, $\lambda = 0.53\,\mu$m) were used to radially compress 200 μm long, 220 μm outer diameter and 20 μm thick polyimide cylinders ($\rho_{poly} = 1.1$ g/cm^3). The tube was filled with CH foam at different densities: 0.1, 0.3 and 1 g/cm^3 and closed on both sides by 20 μm thick foils, made of Ni at the front side and Cu at the rear side. An additional short pulse beam (SP) (5×10^{18} Wcm^{-2}, 10 ps, $\lambda = 1.06\,\mu$m) was focused on the Ni foil to produce fast electrons. In order to prevent the alteration of the SP beam from the low density plasma corona a tube-shaped plastic coated gold shield was stuck onto the Ni foil (see Figure 1). The fast electrons were produced at various times during compression by introducing a delay ($0 \leq \tau \leq 3.5$ns) between SP and LP beams with an accuracy of ± 100 ps (due to the jitter).

The first phase of the experiment was dedicated to the study of the compressed matter's characteristics i.e. the core temperature and density at different stages of the compression. So SP beam was not employed to generate electrons but was used as a backlighting source by focusing it on a Ti foil (25 μm thick) for X-ray radiography diagnostic [4]. The X-ray backlight source placed 10 mm before the target transversally probed the cylinder at different delays during compression. A quartz crystal ($2d = 2.748$Å, $R_c = 380$ mm) situated ~ 200 mm after the target, reflected the Ti Kα radiation (4.5 keV) and imaged the compressed cylinder onto an imaging plate (IP) positioned $\sim$ 2m away with a total magnification of $\sim$ 10.7. The spatial resolution has been calculated with the help of a grid and estimated to $\sim 20\,\mu$m on the target plane. In order to have a better absorption of the X-rays through the cylinder and thus have a better contrast ratio, CH foam was also doped with 30% Cl in mass (for this phase only). In order to predict the evolution of the cylinders' compression simulations have been performed with the 2D hydrodynamic code CHIC [5, 6]. This code, based on a cell-centered Lagrangian scheme, is mainly devoted to numerical simulations of laser driven ICF.

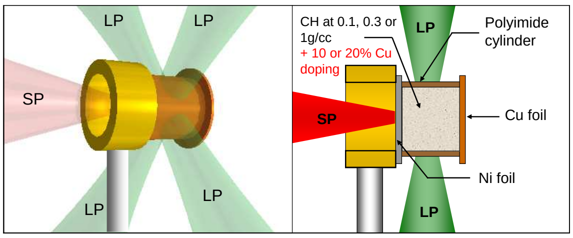

Figure 1. In principle scheme and target.

During the second phase, fast electrons propagation through the compressed cylinder was monitored by the K-shell fluorescence from the Ni and Cu foils. To follow the electrons during their propagation between the two foils CH foam was also doped with 20% Cu in mass (only 10% for 1 g/cm^3 targets). The K-shell fluorescence in the range 7.3 - 9.3 keV was collected by two

Journal of Physics: Conference Series **244** (2010) 022027 doi:10.1088/1742-6596/244/2/022027

X-ray Bragg spectrometers situated at the rear side of the target. The first one was composed by a flat highly oriented pyrolitic graphite (HOPG) [7] crystal with a high reflectivity but low spectral resolution (≈ 50 eV). The second one consisted of a high spectral resolution (≤ 5 eV) cylindrical quartz crystal ($2d = 2.024$Å, $R_c = 100$ mm) in Von Hamos configuration.

3. Experimental results and discussion

During the first phase X-ray radiography allowed us to estimate the core temperatures and densities of the compressed targets. This analysis concerned only 1 g/cm^3 targets. A typical image is presented on Figure 2 (a) representing the compressed cylinder at maximum compression i.e. $\tau = 2.2$ns. It has been possible to simulate the X-ray transmission profile for each delay supposing a laminar flux of X-rays transversally probing a simulated cylinder (2D hydrodynamic simulations).

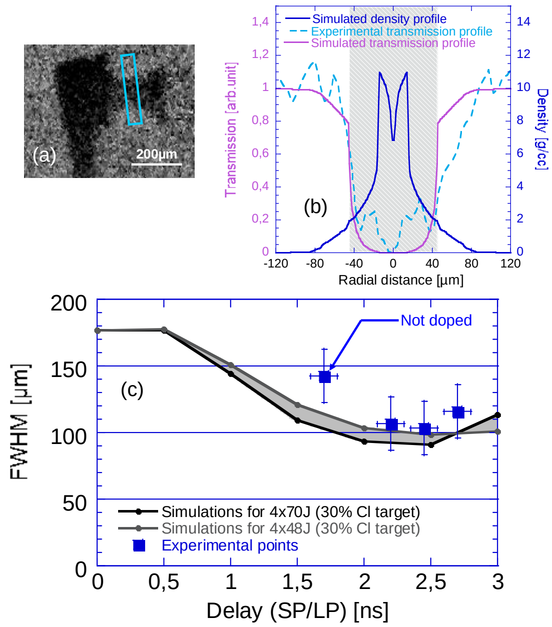

Figure 2. (a) Typical X-ray radiography image obtained for 1 g/cm^3 target at maximum compression (τ =2.2ns). The blue rectangle corresponds to the analyzed area. (b) Experimental vs. simulated transmission profiles of the compressed area. Density is also plotted. The hatched region represents the Cl-doped core (c) Overall results of the X-ray radiography. The grey area corresponds to an uncertainty domain due to energy variations of the LP laser beams.

Figure 2 (b) shows the relatively good agreement between simulated and experimental profile of the transmission obtained for a 1 g/cm^3 target at maximum compression. We can also note that the real radius of the compressed area, given by the density profile, doesn't correspond to the observed radius given by the X-ray transmission profile: $R_{density} \approx 20\,\mu$m $\neq R_{Xray} \approx 45\,\mu$m.

Figure 2 (c) shows the overall results of the X-ray radiography. One can see clearly the compression as a function of the delay and the relatively good reliability of the simulations. It is thus possible to estimate the core temperatures and densities of the 1 g/cm^3 targets (for $4 \times$ 70J LP beams energy) at maximum compression thanks to the simulations:

$$T(2.2\text{ns})_{1\,\text{g/cm}^3} \approx 35\,\text{eV}$$
$$\rho(2.2\text{ns})_{1\,\text{g/cm}^3} \approx 8\,\text{g/cm}^3$$

This good agreement between simulations and experiment for 1g/cc targets allows us to also estimate the core parameters (ρ,T) at maximum compression of 0.1 g/cm^3 and 0.3 g/cm^3 targets with a relatively good confidence:

$$T(1.72\text{ns})_{0.1\,\text{g/cm}^3} \approx 220\,\text{eV}$$
$$\rho(1.72\text{ns})_{0.1\,\text{g/cm}^3} \approx 4\,\text{g/cm}^3$$
and
$$T(1.9\text{ns})_{0.3\,\text{g/cm}^3} \approx 80\,\text{eV}$$
$$\rho(1.9\text{ns})_{0.3\,\text{g/cm}^3} \approx 4\,\text{g/cm}^3$$

During the second phase the two Bragg spectrometers detected the Ni and Cu emission looking at the target's rear side. The Kα and Kβ fluorescence yields from the Ni foil on the front side of the cylinder are interpreted as a signature of the fast electrons source. The Cu-Kα fluorescence yields emitted either from the Cu doped CH foam or from the rear side Cu layer were used as a diagnostic of the fast electrons propagation

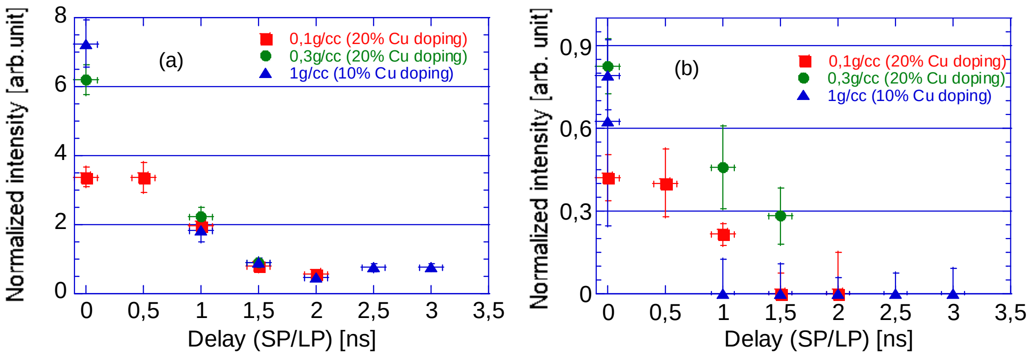

Figure 3. (a) Overall results from the HOPG spectrometer: Cu-Kα/Ni-Kβ ratio as a function of the Delay τ (b) Overall results from the Von-Hamos spectrometer: Cu-Kα/Ni-Kα ratio as a function of the Delay τ . The Cu-Kα/Ni-K$\beta(\alpha)$ ratio corresponds to the relative quantity of electrons that reached the rear side Cu foil divided by the relative quantity of electrons that are generated on the front side Ni foil.

range. A compilation of the results obtained with the HOPG spectrometer is presented in Figure 3 (a). To account for the small shot-to-shot variations of the fast electrons source, the Cu-Kα yields were adjusted to the Ni-Kβ yields for each shot. The Cu-Kα/Ni-Kβ ratio is used as a normalized measure of the fraction of the hot (> 8 keV) electrons reaching the rear surface of the target. We clearly observe a decrease of the ratio against SP/LP delay i.e. against compressed foam density. It means that electrons are slowed down more efficiently when the density grows up. However one can not observe a clear dependence on the initial foam density. Results from the Von Hamos spectrometer confirm these trends (see Figure 3 (b)).

4. Conclusion

The first phase was devoted to the characterization of the compression. With the help of the X-ray radiography diagnostic it has been possible to observe the cylinder's compression as a function of the time. Comparison of the experimental results with the 2D hydrodynamic simulations from CHIC allowed us to estimate the core temperature and density of the compressed target taking into account laser beam energy variations.

In order to study the fast electrons propagation the second phase was monitored by two X-ray spectrometers analysing the K-shell emission from the compressed targets. For all the tested initial target densities, the fraction of the fast electrons population reaching the cylindrical targets rear side decrease during compression. 2D hybrid simulations of the fast electrons transport are still underway in order to explain this behaviour.

5. Acknowledgments

This experiment is a part of the HiPER experimental roadmap and has been fully supported by the HiPER project.

References

[1] Tabak M *et al* , 1994 *Phys. Plasmas* **1** 1626-1634
[2] Atzeni S *et al* , 2008 *Phys. Plasmas* **15**, 056311
[3] Nakamura H *et al* , 2008 *Phys. Rev. Lett.* **100**, 165001
[4] Aglitskiy Y *et al* , 1998 *App. Opt.* **37**, 5253-5261
[5] Maire P H and Breil J, 2008 *Int. J. Nummer. Methods Fluids* **56**, 1417-23
[6] Maire P H *et al* , 2007 *SIAM J. Sci. Comput.* **29**, 1781
[7] Pak A *et al* , 2004 *Rev. Sci. Instr.* **75**, 3747-3749